Fluorene and Phenanthrene Uptake by *Pseudomonas putida* ATCC 17514: Kinetics and Physiological Aspects

Ana C. Rodrigues,[1] Stefan Wuertz,[2] António G. Brito,[1] Luís F. Melo[3]

[1]University of Minho, Centre of Biological Engineering, 4710-057 Braga, Portugal; telephone: (351)253604400; fax: (351)253678986; e-mail: acrodrigues@deb.uminho.pt
[2]Institute of Water Quality Control and Waste Management, Technical University of Munich, Am Coulombwall, D-85748 Garching, Germany
[3]LEPAE – Faculty of Engineering of the University of Porto, Chemical Engineering Department, 4200-465 Porto, Portugal

Received 7 July 2004; accepted 14 October 2004

Published online 30 March 2005 in Wiley InterScience (www.interscience.wiley.com). DOI: 10.1002/bit.20377

Abstract: *Pseudomonas putida* ATCC 17514 was used as a model strain to investigate the characteristics of bacterial growth in the presence of solid fluorene and phenanthrene. Despite the lower water-solubility of phenanthrene, *P. putida* degraded this polycyclic aromatic hydrocarbon (PAH) at a maximum observed rate of 1.4 ± 0.1 mg L^{-1} h^{-1}, higher than the apparent degradation rate of fluorene, 0.8 ± 0.07 mg L^{-1} h^{-1}. The role of physiological processes on the biodegradation of these PAHs was analyzed and two different uptake strategies were identified. Zeta potential measurements revealed that phenanthrene-grown cells were slightly more negatively charged (-57.5 ± 4.7 mV) than fluorene-grown cells (-51.6 ± 4.9 mV), but much more negatively charged than glucose-grown cells (-26.8 ± 3.3 mV), suggesting that the PAH substrate induced modifications on the physical properties of bacterial surfaces. Furthermore, protein-to-exopolysaccharide ratios detected during bacterial growth on phenanthrene were typical of biofilms developed under physicochemical stress conditions, caused by the presence of sparingly water-soluble chemicals as the sole carbon and energy source for growth, the maximum value for TP/EPS during growth on phenanthrene (1.9) being lower than the one obtained with fluorene (5.5). Finally, confocal laser microscopy observations using a *gfp*-labeled derivative strain revealed that, in the presence of phenanthrene, *P. putida::gfp* cells formed a biofilm on accessible crystal surfaces, whereas in the presence of fluorene the strain grew randomly between the crystal clusters. The results showed that *P. putida* was able to overcome the lower aqueous solubility of phenanthrene by adhering to the solid PAH throughout the production of extracellular polymeric substances, thus promoting the availability and uptake of such a hydrophobic compound.

Correspondence to: Ana Cristina Rodrigues

Current address for S. Wuertz: Department of Civil and Environmental Engineering, University of California, Davis, One Shields Ave., Davis CA, 95616, USA.

Contract grant sponsors: Foundation for Science and Technology/ M.C.T., Portugal; EC Biotech program

Contract grant numbers: PRAXISXXI/BD/15944/98 (to A.C.R.); BIO4-CT97-2015

Keywords: fluorene; phenanthrene; biodegradation; CLSM; GFP

INTRODUCTION

Fluorene and phenanthrene are among the most common polycyclic aromatic hydrocarbons (PAHs) found at contaminated industrial sites (George and Neufeld, 1989; Bezalel et al., 1996). The microbial uptake kinetics of such compounds is constrained by their solid physical state and very low water-solubility, leading to their accumulation in the environment (Cerniglia, 1992; Wodzinski and Coyle, 1974). Some microorganisms are able to adapt to hydrophobic PAHs by using efficient substrate-to-cell contact mechanisms and several studies pointed out the relevance of adhesion in substrate bioavailability. Guerin and Boyd (1992) found that desorption of soil-sorbed naphthalene was enhanced by a *Pseudomonas putida* strain, which strongly adhered to the sorbent surface. Likewise, Wick et al. (2002) indicated attachment and biofilm formation as a specific physiological response of *Mycobacterium sp.* LB501T to optimize anthracene bioavailability. However, no specific information regarding bacterial adaptations, such as the production of polymeric substances as a substrate-induced bioavailability-enhancing mechanism was clearly provided.

Therefore, in order to better understand strain-specific mechanisms to improve PAH bioavailability, more knowledge about bacterial physiological processes affecting the uptake of different substrates is necessary. An appreciation of the mechanisms that control PAH biodegradation will be very helpful in developing practical bioremediation strategies. Thus, the goal of the present work was to identify specific responses of *P. putida* ATCC 17514 to different sparingly soluble PAHs, namely, fluorene and phenanthrene. For that purpose, the kinetics of fluorene and

phenanthrene utilization as the sole carbon and energy source for growth were determined, the role of biopolymer production and bacterial surface properties in PAH uptake mechanism was analyzed, and the growth strategy of gfp-labeled *P. putida* ATCC 17514 on fluorene and phenanthrene crystals was identified in situ using confocal laser scanning microscopy.

MATERIALS AND METHODS

Chemicals

Fluorene (FL; 98% pure) was purchased from Sigma Aldrich (Steinheim, Germany) and phenanthrene (PHE; 98% pure) was purchased from Aldrich Chemical (Milwaukee, WI). PAH stock solutions (10 mg mL^{-1}) were prepared by dissolution of fluorene or phenanthrene crystals in acetone or n-hexane (Riedel-de-Häen).

Bacteria and Culture Conditions

Pseudomonas putida ATCC 17514 NCIMB 10015 was first grown in mineral medium with glucose (2 g/L) for 24 h at 25°C. The mineral medium contained, per liter of solution: 69.6 mg of $CaCl_2.2H_2O$, 8 mg of NaCl, 103 mg of KNO_3, 698 mg of $NaNO_3$, 100 mg of $MgSO_4.7H_2O$, 100 mg of NTA, 2 mg of $FeSO_4.7H_2O$, 0.1 mg of $ZnSO_4.7H_2O$, 0.043 mg of $MnSO_4.5H_2O$, 0.3 mg of H_3BO_3, 0.24 mg of $CoSO_4.7H_2O$, 0.01 mg of $CuSO_4.5H_2O$, 0.02 mg of $NiSO_4.7H_2O$, 0.03 mg of $NaMoO_4.2H_2O$, 0.5 mg of $Ca(OH)_2$, 5 mg of EDTA, 544.4 mg of KH_2PO_4, 2148.9 mg of Na_2HPO_4, and 30 mg of $(NH_4)_2SO_4$. Subsequently, fluorene or phenanthrene crystals were added to the medium for enzyme induction. The cultures were then incubated for 7 days in the dark at 25°C, with shaking at 150 rpm. *P. putida* was able to use fluorene or phenanthrene as the sole carbon and energy source for growth.

A double *gfp* cassette, containing two copies of *gfp* with the strong *psbA* constitutive promoter plus a ribosome binding site from T7gene10 was used to label *P. putida* ATCC 17514. Plasmid pUTgfp2 (Unge et al., 1996) is a transposon delivery system used for stable chromosomal integration of two copies of *gfp*, consisting of a mutant form of GFP, which is excited at 471 nm (instead of 396 nm) and more prominently expressed compared to the wildtype GFP. The plasmid pUTgfp2 was transferred by conjugation from a donor strain, *E. coli* DH5α, to *P. putida* ATCC 17514 in a triparental mating with helper strain CM404, which is HB101 carrying the necessary transfer genes for conjugation on plasmid pRK2013 (Figurski and Helinski, 1979).

Escherichia coli strains were grown at 37°C in Luria-Bertani (LB) medium supplemented with ampicillin (50 μg/mL) or kanamycin (50 μg/mL), for DH5α and CM404, respectively. *P. putida* (wildtype and *gfp*-tagged) cells were incubated at 30°C on agar plates (Pseudomonas Agar Base, OXOID) using mineral medium with gluconate as carbon source, supplemented with kanamycin (50 μg/mL).

Since the wildtype *P. putida* is also resistant to kanamycin (50 μg/mL), fluorescent colonies were detected in a dark room upon exposure to an UV lamp (312 nm) and the colony with the highest fluorescence intensity was scraped off the agar plate and restreaked several times on agar plates with mineral medium supplemented with kanamycin (50 μg/mL), using gluconate as the carbon source.

Biodegradation Assays

Experiments to measure the removal rates and the partition coefficients of PAHs between the solid phase and the liquid phase were carried out in 250-mL Erlenmeyer flasks. PAH-containing medium was prepared by adding a 500-μL aliquot of acetone-dissolved fluorene or phenanthrene (10 mg mL^{-1}) to sterile Erlenmeyer flasks. The solvent was allowed to evaporate before the addition of 50 mL of sterile mineral medium, corresponding to a final PAH content of ~100 mg L^{-1}. The inoculum was a culture of *P. putida* ATCC 17514 pregrown on the respective PAH (with an optical density at 540 nm (OD_{540}) of 0.4). The volume of the inoculum was 10% of the total liquid volume. A flask with only mineral medium was also inoculated and used as control. After inoculation, the flasks were sealed with sterile silicone stoppers, from which a gas filter was suspended and incubated in the dark at 24°C on a gyratory shaker at 150 rpm for 10–15 days. A 2-mL aliquot of cell suspension was sampled at regular time intervals and its OD_{540} was determined as a measure of the density of cell suspensions, after carefully shaking the samples. The OD_{540} was measured in a UNICAM, HEΛIOS γ spectrophotometer (Cambridge, UK), using a cell-free control as reference. Due to their size (0.2–0.5 mm, as evaluated by confocal laser scanning microscopy), PAH crystals sedimented quickly and did not interfere with the OD measurements. Volatile suspended solids concentration was determined as a measure of biomass concentration. Measurements were carried out as described in APHA (1998).

Sterile uninoculated and autoclaved controls were included. In order to determine the effect of bacterial cell surfaces on adsorption to solid PAHs, experiments with inactivated biomass were performed. A cell suspension of *P. putida* was inactivated by autoclaving (121°C, 1.5 bar) for 1 h, followed by a second autoclaving step (15 min) the next day (Hwu et al., 1996). Inactivated cell suspension (OD_{540} = 0.4) was added to Erlenmeyer flasks containing 50 mL of sterile mineral medium, and fluorene or phenanthrene as sole substrates (~100 mg L^{-1}). The sterility of the medium was confirmed by plating in solid LB medium.

The concentration of PAH in the samples was determined. Some samples were clarified by centrifugation at 16,000*g* for 10 min in order to quantify PAH in the solid phase (solid substrate and cell-associated fraction), as well as the PAH in the liquid phase. The supernatant was

transferred to a sterile tube and the pellet was resuspended in 1 mL of mineral medium.

The partition coefficients of PAH between the solid phase and the liquid phase were calculated from the slope of a plot of pellet PAH content (mg_{PAH}/g_{VSS}) versus PAH concentration in the liquid phase (mg_{PAH}/L).

Activity Tests

The specific activity of *P. putida* cells was measured by respirometry at different stages of fluorene and phenanthrene degradation assays using a Biological Oxygen Monitor (YSI model 5300). The respirometry test device had a volume of 10 mL and was sealed with a tightly fitting stopper. The suspension was mixed with a magnetic stirrer to overcome external mass transfer resistance. Oxygen depletion was monitored continuously by using a YSI electrode. The batch respirometric experiments were performed at room temperature (~24°C) during 14 days of *P. putida* growth on fluorene or phenanthrene as sole substrates, as follows: 10 mL of growth medium were saturated with oxygen by air bubbling and stirring for 30 min, the respirometric cell was closed, and oxygen consumption was monitored. Mineral medium without added PAH, inoculated with *P. putida* cells, was used as control. The maximum specific activity was calculated from the oxygen consumption curve.

In Situ Monitoring by CLSM of Bacterial Growth on Sorbed PAHs

Growth experiments with the *gfp*-labeled derivative strain of *P. putida* ATCC 17514 on PAHs sorbed to a glass surface were carried out in a four-channel (5 × 10 × 40 mm) flow-cell, limited by two microscope glass coverslips. The glass coverslip at the bottom of the flow-cell was coated with PAH crystals (0.2–0.5 mm). In channels 1 and 2, a single PAH was used (phenanthrene in channel 1 and fluorene in channel 2). In channel 3, fluorene was placed at the inlet and phenanthrene at the outlet. The glass surface area coated with PAH crystals (at the inlet and at the outlet of each flow channel) was approximately equivalent to 2 mm^2. The flow cell was filled up with a flow of mineral medium. Thereafter, each flow channel was inoculated with a culture of *gfp*-labeled *P. putida* cells (OD_{540} = 0.4) pregrown on the respective PAH, as described for the biodegradation experiments. After 1 h of incubation, mineral medium was continuously pumped at a flow rate of 5 mL h^{-1}.

The flow-cell was placed under a microscope AXIOVERT 135 TV with a confocal laser unit, coupled to a Leica QUANTIMET image analysis computer. In each channel, three distinct areas, at the inlet (a), at the middle (b), and at the outlet (c), were monitored. Twenty horizontal optical sections were scanned at 2-μm vertical intervals. The bacteria were detected with an Ar 488 nm laser using a 515 nm long-pass filter, and the PAH crystals with a HeNe 543 nm laser line using a 550 nm long-pass filter. Images were obtained using a 40×/1.3 oil immersion lens. The growth of *P. putida*::gfp cells was monitored for 6 days and biovolumes were determined by numeric integration of microbial colonization profiles, following the method described in Kuehn et al. (1998). The flow cell system was kept under the CLSM for the entire experimental period so that the same site was always scanned. The room temperature was 18°C.

PAH Analysis

Each sample was extracted with two equal volumes of n-hexane. A centrifugation (16,000*g* for 10 min) was performed to separate aqueous and organic phases. PAHs in the hexane fraction were separated by reversed-phase high-pressure liquid chromatography (RP-HPLC) analysis using a Knauer chromatograph, equipped with a Knauer K-2500 UV-detector (254 nm). A LiChroCART 250-4 LiChrospher PAH column was used for component separation. The compounds were eluted using a gradient of acetonitrile (A) and water (0–10 min, 50%A; 10–35 min, 100%A), pumped at a flow-rate of 1 mL/min by using a solvent organizer K-1500 WellChrom, Knauer and a HPLC pump K-1001, WellChrom, Knauer. Total PAH concentrations were determined from a mixed liquor sample (containing mineral medium, cells, solid and dissolved PAHs). PAH in the solid phase (solid PAH and cell-associated PAH) and PAH concentration in the liquid phase (dissolved PAH and very small PAH crystals) were determined after centrifugation of the mixed liquor sample (16,000*g* for 10 min). The supernatant was transferred to a sterile tube and the pellet was resuspended in 1 mL of mineral medium. For quantification of PAH in the solid phase, the sample was previously sonicated for 2 min, in order to allow the detachment of cells from insoluble PAH, and afterwards extracted with n-hexane.

Biopolymers

Cell production of biopolymers was assessed during PAH degradation assays. A quantitative approximation of the exopolysaccharide (EPS) matrix was obtained using the phenol-sulfuric acid method of Dubois et al. (1956). Glucose was used as standard and the absorbance was measured at 490 nm in a UNICAM, HEλIOS γ spectrophotometer. The total protein (TP) concentration was measured according to the Lowry et al. (1951) method with a kit supplied by Sigma (St. Louis, MO, procedure 5656), using bovine serum albumin as standard. Absorbance was measured at 740 nm.

Cell Surface Properties

Relative cell surface hydrophobicity determinations were carried out using a modification of the method described by

Rosenberg et al. (1980). *P. putida* ATCC 17514 was grown in batch cultures, as described above, and harvested at the early stationary growth phase by centrifugation (12,000*g*, 10 min). The pellet was washed, resuspended, and diluted with mineral medium to an initial OD_{540} of 0.4. The purity of the cultures was confirmed by plating on LB medium. A 4.5 mL portion of cell suspension (OD_{540} = 0.4) was transferred to an acid-washed (HCl, 0.1 M) round-bottom glass tube, previously overlaid with 0.6 mL of hexadecane. For each culture, one control (tube not overlaid with hexadecane) was prepared. Samples and controls were then vortexed for 60 sec. After an equilibration period of 10 min, the loss in OD_{540} of the aqueous phase relative to that of the initial cell suspension was measured. Hydrophobicity was estimated by calculating the percentage of cells adhering to hexadecane. The electric charge of *P. putida* cells grown on fluorene or phenanthrene was evaluated by zeta potential determinations. Measurements were performed with a micro-electrophoresis cell, Zetameter 3.0+. The applied voltage was 200 V, and each average value consisted of 25 records.

RESULTS

Kinetics of PAH Biodegradation

Degradation and growth experiments with *P. putida* ATCC 17514 were performed in batch cultures using either crystalline fluorene or phenanthrene as sole carbon and energy sources. The results are presented in Figures 1 and 2.

After an equilibration period, fluorene and phenanthrene concentrations in the suspension decreased with time. During the exponential growth phase, the partitioning of the PAH to the cells was observed as a significant increase in the concentration of PAH in the solid phase. Concomitantly, the PAH concentration in the bulk liquid decreased. Afterwards, at the late exponential growth phase, the PAH concentration in the solid phase declined continuously as a result of the continued metabolism of cell-associated PAH. The maximum observed degradation rates are depicted in Table I, the phenanthrene degradation rate being higher than with fluorene. Furthermore, biological activity during growth on phenanthrene (1.16 g O_2 g VSS^{-1} d^{-1}, at the exponential phase) was much higher than on fluorene (Fig. 3). Apparently, the maximum cell activity was reached when most of the phenanthrene was associated with the biomass (as can be seen in Fig. 2). No cell activity was detected in the absence of fluorene or phenanthrene as substrate.

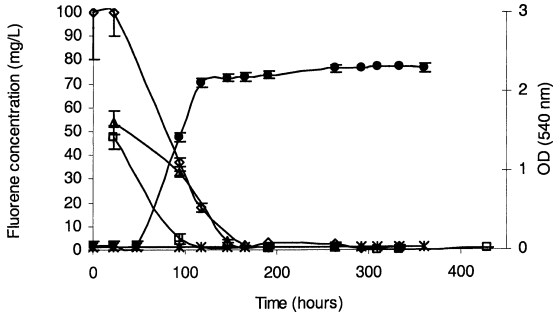

Figure 1. Removal of total fluorene (◇), fluorene in the bulk liquid phase (□) and fluorene in the solid phase (△) during growth of *P. putida* ATCC 17514 (●). The lack of biomass growth in the absence of fluorene is also depicted (∗). The error bars represent the standard deviation calculated on the basis of measurements performed in two experiments.

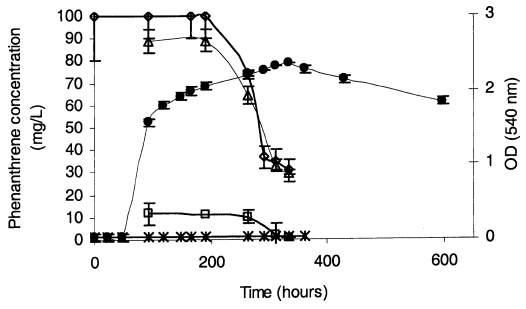

Figure 2. Removal of total phenanthrene (◇), phenanthrene in the bulk liquid phase (□) and phenanthrene in the solid phase (△) during growth of *P. putida* ATCC 17514 (●). The lack of biomass growth in the absence of phenanthrene is also depicted (∗). The error bars represent the standard deviation calculated on the basis of measurements performed in two experiments.

The effect of cell-surface properties in PAH association with the biomass was investigated in batch assays performed with inactivated cells (Table I). The increase in PAH in the solid phase and the simultaneous inflection in the concentration of PAH in the liquid phase was more noticeable for phenanthrene. These data are consistent with the slightly higher hydrophobicity of this PAH compared to fluorene, since the water-solubility of the two compounds differs by a factor of 1.6.

Cell Surface Properties and Bacterial Production of Biopolymers

The effect of the growth substrate on the physical properties of bacterial surfaces was also analyzed. After *P. putida* growth on fluorene, phenanthrene, or glucose, measurements of zeta potential and bacterial surface hydro-

Table I. Maximum observed degradation rates and partition coefficients.

PAH	Maximum observed degradation rates (mg L^{-1} h^{-1})	Initial partition coefficients in the presence of active cells (L g VSS^{-1})	Initial partition coefficient in the presence of inactive cells (L g VSS^{-1})
Fluorene	0.8 ± 0.07	3.0 ± 0.9	4.6 ± 0.5
Phenanthrene	1.4 ± 0.1	10.5 ± 1.8	18.5 ± 1.2

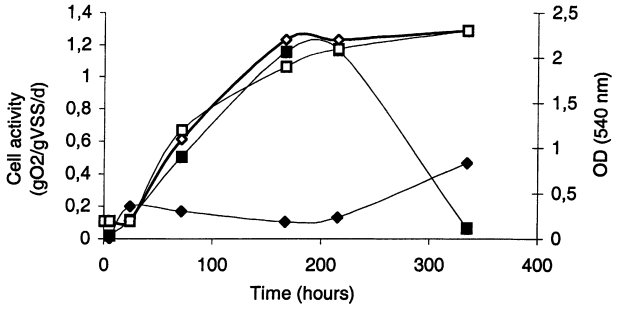

Figure 3. Activity of *P. putida* cells during growth on fluorene (♦) or phenanthrene (■). The optical density of the medium at 540 nm is also represented as a measure of biomass growth on fluorene (◇) or phenanthrene (□).

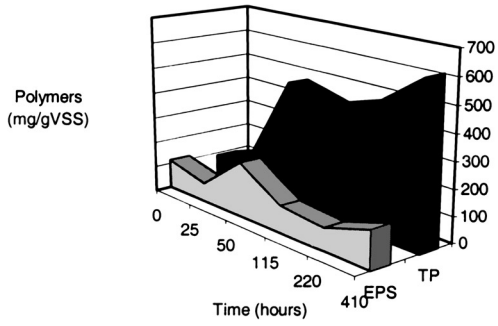

Figure 4. Biopolymer production during growth on fluorene.

phobicity were performed in order to examine whether the used carbon source affects the cell surface properties (Table II).

As expected, zeta potential measurements revealed that the strain was always negatively charged at neutral pH (Table II), although the growth substrate was different. Cells grown on glucose were the least charged, while cells grown on PAHs displayed extremely high negative zeta potential values. However, despite the slightly higher hydrophobicity and more negative electric charge of cells grown on phenanthrene compared to fluorene, no significant differences were registered between cells grown on these substrates.

The production of biopolymers, namely, exopolysaccharides (EPS) and total proteins (TP), during bacterial growth on fluorene and phenanthrene is shown in Figures 4 and 5, respectively. After an adaptation period, an increase in the concentration of biopolymers was observed. In general, the ratio of total protein to exopolysaccharides was lower in the presence of phenanthrene compared to fluorene (Fig. 6), which means that the production of polysaccharides was higher in the presence of phenanthrene crystals.

In Situ CLSM Monitoring of Bacterial Growth on Sorbed PAHs

In order to monitor the growth of *P. putida* ATCC 17514 on fluorene and phenanthrene crystals using confocal laser scanning microscopy, the strain was labeled by transposon mutagenesis. *P. putida*::gfp cells were found to express strong, green fluorescence, clearly detectable by epifluorescence or confocal microscopy. During all flow-cell experiments, expression of GFP was very stable and no nonfluorescent subpopulations were observed.

After inoculation and an adaptation period of about 24 h, growth of *P. putida*::gfp cells was detected in all scanned regions in channels 1 (phenanthrene crystals only) and 2 (fluorene crystals only). On the other hand, in channel 3 (inlet: fluorene, outlet: phenanthrene), a confluent growth of *P. putida* cells was observed near the outlet, i.e., where the phenanthrene crystals were located, and nearly no cells could be detected at the inlet and at the center of the channel. Figure 7 shows *P. putida* cell distribution in channels 1 (image A) and 2 (image B).

Table II. Cell-surface characteristics of *Pseudomonas putida* ATCC 17514 grown on different substrates.

Growth substrate	Zeta potential (mV)	% cells adhered to hexadecane
Fluorene	−51.6 ± 4.9	4.7 ± 0.7
Phenanthrene	−57.5 ± 4.7	6.2 ± 0.5
Glucose	−26.8 ± 3.3	—

DISCUSSION

Kinetics of Fluorene and Phenanthrene Biodegradation

Degradation and growth experiments with *P. putida* ATCC 17514 were performed in batch cultures using either crystalline fluorene or phenanthrene as the sole carbon and energy sources, at a concentration of 100 mg L^{-1}. Such initial PAH concentration was much higher than the PAH aqueous solubility limit in order to ensure that PAH dissolution from crystals was never the limiting step of biomass growth. Figures 1 and 2 show that, after a lag

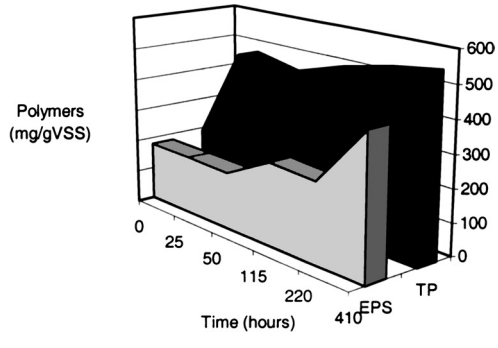

Figure 5. Biopolymer production during growth on phenanthrene.

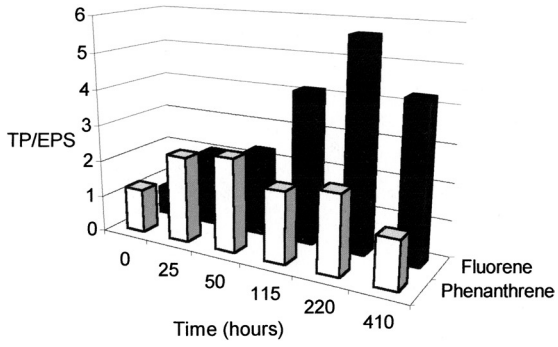

Figure 6. Comparison of the ratio between total protein and polysaccharides during *P. putida* growth on fluorene and on phenanthrene crystals.

period of ~48 h, exponential growth was observed only at high substrate-to-microorganism ratios. In all experiments it was noticed that cultures in the presence of fluorene reached the stationary growth phase before those grown on phenanthrene. During the exponential growth phase, the observed growth rate in the presence of fluorene was 0.0196 h^{-1}. After 120 h of incubation, the growth rate decreased to 0.0005 h^{-1}. With phenanthrene (Fig. 2), the growth was clearly characterized by two distinct stages: an exponential phase with an observed growth rate of 0.0317 h^{-1}, followed by a linear growth (at a rate of 0.0018 h^{-1}). At high biomass concentrations (around 1.1 g_{VSS}/L), phenanthrene aqueous solubility limit appears to be the limiting step controlling the uptake rate. The observed growth rate in the presence of solid phenanthrene was approximately one-half of the rate obtained by Boldrin et al. (1993) during the exponential growth of a *Mycobacterium* sp., using the same substrate (0.069 h^{-1}). This difference can be explained by the strong hydrophobicity and very high adhesion efficiency usually exhibited by *Mycobacterium* spp (Bastiaens et al., 2000), properties that are believed to be favorable to the biodegradation of sorbed PAHs (Wick et al., 2002).

During biodegradation assays, it was observed that, either for fluorene or phenanthrene, most of the PAH-compound was present in the suspension as solid PAH and/or cell-associated PAH. Indeed, after 100 h of *P. putida* growth on fluorene, 63.0 ± 20.3% of the total PAH was localized in the solid fraction. On the other hand, 90.1 ± 9.4% of the total PAH was solid and/or associated to the cells during growth on phenanthrene. This trend is again consistent with the higher hydrophobicity of phenanthrene and its affinity for lipid membranes.

The initial partition coefficients between the solid phase and the supernatant, obtained for fluorene and phenanthrene were 3.0 ± 0.9 and 10.5 ± 1.8 L g VSS^{-1}, respectively. These values for the partition coefficients determined are conservative. In fact, due to the active degradation of the substrate by the cells, the experimental results tend to indicate the combined effects of transport to the cells and metabolism of cell-associated PAH. In the presence of inactivated cells, the initial partition coefficients (Table I) are higher than the ones obtained with active biomass (4.6 ± 0.5 and 18.5 ± 1.2 L g VSS^{-1}, for fluorene and phenanthrene, respectively). This result confirms that the values for the partition coefficients determined with active biomass are underestimated due to PAH metabolism and suggests that there is a spontaneous partitioning of fluorene and phenanthrene to the cells as a result of their lipophilic nature and hydrophobicity, although the higher concentration of PAH in the solid phase is also due to PAH crystals that were centrifuged out of suspension along with cells during the experimental procedure described in Materials and Methods.

The maximum specific fluorene and phenanthrene apparent degradation rates were 12.9 ± 0.3 and 17.5 ±

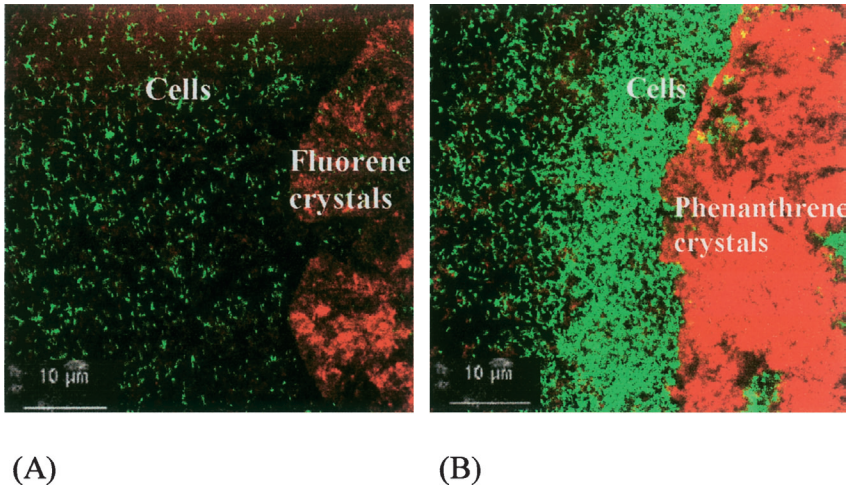

Figure 7. On-line monitoring of the growth of *P. putida*::gfp cells on crystalline fluorene and phenanthrene. Each image is presented as a horizontal cross section through a microcolony of cells located near the fluorene (**A**) and phenanthrene (**B**) crystals. GFP-expressing cells are green and the red signal refers to the PAH crystals.

0.7 mg PAH g VSS^{-1} d^{-1}, corresponding to 0.8 ± 0.07 and 1.4 ± 0.1 mg L^{-1} h^{-1}, respectively. Despite the lower solubility in water of phenanthrene, *P. putida* seemed to degrade this PAH at a rate slightly higher than fluorene. The results obtained in the biodegradation experiments indicated that the low bioavailability of phenanthrene caused by its low aqueous solubility could be overcome. Therefore, the contribution of physiological mechanisms, such as biopolymer production to promote bacterial adhesion to sparingly soluble PAHs, thus improving the bioavailability of such hydrophobic substrates, was highlighted.

Effect of the Substrate Type on the Physical Properties of Cell Surface

The hydrophobicity measurements showed that *P. putida* is rather hydrophilic. However, some influences of the substrate on the physical properties (hydrophobicity and zeta potential) of bacterial surfaces were observed (Table II). Zeta potential values were significantly different when comparing cells grown on PAHs and on a more easily degradable carbon source (glucose). The results showed that PAH-grown cells were more negatively charged (–51.6 ± 4.9 to –57.5 ± 4.7 mV) than glucose-grown cells (–26.8 ± 3.3 mV). This difference could be attributed to a modification of the cell surface of the bacteria. Wick et al. (2002) also reported differences in surface properties of a *Mycobacterium* strain according to the substrate regime, glucose-grown cells being slightly larger, significantly more hydrophilic, and less negatively charged than anthracene-grown cells.

The zeta potential value measured for *P. putida* cells pregrown on glucose (–26.8 ± 3.3 mV) is similar to the one obtained by Bastiaens et al. (2000) with the naphthalene-degrading *P. putida* strain PpG7 (Dunn and Gunsalus, 1973) during growth on the same easily degradable carbon source (–32.06 ± 5.23 mV). Furthermore, in the presence of fluorene or phenanthrene, *P. putida* cells displayed an extremely high negative charge (–51.6 ± 4.9 and –57.5 ± 4.7 mV, respectively), only slightly lower than the electric cell surface charge exhibited by a hydrophobic strain belonging to the *Mycobacterium* genus (–66 mV), as reported by the same authors. This result suggests that, particularly during growth on phenanthrene crystals, the characteristics of bacterial surface are similar to the ones displayed by the referred *Mycobacterium* strain, which presents a very strong adhesion capacity.

In fact, despite the high negative zeta potentials of *P. putida* cells detected during growth on PAHs, the formation of cell aggregates could be observed. This observation is in apparent contradiction with the high electrostatic repulsion expected to occur between highly negatively charged cells. The adhesion capacity is inversely correlated to a high negative surface charge (Oliveira, 1992). The observed formation of cell aggregates is explained by favorable polymer interactions.

The surface of cells grown on phenanthrene was slightly more negatively charged (57.5 ± 4.7 mV) than the surface of cells grown on fluorene (–51.6 ± 4.9 mV). It is known that, for relatively hydrophilic cell surfaces, the electrokinetic potential becomes more influential on bacterial adhesion (van Loosdrecht et al., 1987). These differences in the zeta potential values may be related to the type and concentration of exopolysaccharides excreted by *P. putida* cells during growth on these PAHs. The EPS synthesized by microbial cells vary in their chemical and physical properties (Sutherland, 2001). Those organic molecules (proteins and complex polysaccharides) conditioning the cell surface will change the surface charge of the original surface, as determined by zeta potential measurements (Neu, 1996).

Cell Production of Polymeric Substances

The concentration of total polysaccharides and proteins was assessed during *P. putida* growth on fluorene and phenanthrene crystals. A higher cell production of biopolymers was observed in the presence of phenanthrene compared to fluorene (Figs. 4, 5). Moreover, there was a clear difference in the composition of the biomass during growth on both substrates (Fig. 6). In fact, in the presence of fluorene, the ratio of total protein to exopolysaccharides (TP/EPS) increased continuously, reaching a maximum value of 5.5 on day 9. On the other hand, with phenanthrene, the maximum value for the protein to exopolysaccharides ratio, 1.9, was observed during day 2, after which it decreased to a lower value (between 0.5 and 1.2). This ratio of total protein to exopolysaccharides (TP/EPS) was the parameter used by Lazarova et al. (1994) to determine the structure and solidity of biofilms. According to these authors, the higher TP/EPS values observed in the presence of fluorene correspond to homogeneous, smooth, and fragile biofilms, whereas TP/EPS values of 0.5 to 2.0, detected during bacterial growth on phenanthrene, are typical of biofilms developed under physicochemical stress conditions, which often present a much stronger exopolysaccharide matrix. Lopes et al. (2000) obtained a maximum value for the protein to exopolysaccharides ratio of 25.6 during growth of *P. fluorescens* on glucose in an airlift reactor. Despite the strong hydrodynamic forces that prevail in such a system, the results indicate that PAHs are likely to exert more stress than glucose. Furthermore, phenanthrene-grown cells are submitted to stronger stress conditions than fluorene-grown cells. Therefore, the biosynthesis and release of polymeric substances can be a bacterial strategy to promote bioavailability of less water-soluble compounds and/or adhesion to hydrophobic surfaces.

The adhesion of bacterial cells to PAHs is greatly determined by the physical properties of the macromolecules at the cell surface, the formation of bridges of extracellular polymers being responsible for anchoring the cells to the substratum. According to Rattee and Breuer

(1974), the binding interaction between a dye and cellulosic polymers occurs by hydrogen bonding between the pyranose rings of the polysaccharide and the aromatic rings of the dye. The same kind of interaction may occur between EPS and PAHs. Possibly, PAHs adsorb to or interact via hydrogen bonding with EPS, thereby becoming more available to the cells in the biofilm. Such enhanced bioavailability can be explained by a reduction of the PAH diffusion pathway (between the bulk liquid and the biofilm) and a sharp substrate concentration gradient, caused by the adhered bacteria, which may in turn enhance the diffusive substrate flux. Moreover, many biosurfactants/bioemulsifiers are just complex structures of polysaccharides and proteins, which are known to increase the apparent solubility of hydrophobic compounds (Barkay et al., 1999; Burd and Ward, 1996).

In Situ CLSM Monitoring of Bacterial Growth on Sorbed PAHs

Cell growth was detected microscopically based on GFP fluorescence in the presence of fluorene, phenanthrene, or both PAHs, as the sole carbon and energy source. *P. putida* seems to use different growth strategies according to the PAH it is feeding on. In fact, *P. putida*::gfp cells attached and grew on the phenanthrene crystals, forming a biofilm over accessible surfaces (Fig. 7). On the other hand, in the presence of fluorene, which is more water-soluble than phenanthrene, CLSM observations showed that the strain grew randomly between the crystal clusters feeding on the dissolved PAH. Moreover, in the presence of both PAHs, *P. putida* directly colonize phenanthrene crystals in order to reduce the PAH diffusion pathway and to take advantage of the higher substrate concentration at the surface crystal, despite the fact that they can also feed on the available fraction of fluorene, which is being dissolved. The different growth patterns exhibited by *P. putida* ATCC 17514 can be attributed to the differences in substrate properties. Indeed, by adhering to phenanthrene throughout the formation of a biofilm, *P. putida* cells may be favored to utilize the insoluble PAH compound, being able to overcome its lower aqueous solubility. Biofilm formation by a *Mycobacterium* strain on solid anthracene was also detected by Wick et al. (2002). The same authors suggest that biofilm formation may be required for growth under conditions of low substrate availability.

In conclusion, the results obtained in the present study revealed different growth strategies of a *P. putida* strain on fluorene and phenanthrene crystals, showing that PAH uptake strategy depends on bacterial strain-specific mechanisms which are induced by the physical and chemical characteristics of the PAH compound. Indeed, despite the lower aqueous phase phenanthrene concentration *P. putida* ATCC 17514 was able to utilize this PAH compound at a rate higher than the one observed for fluorene by adhering to the solid substrate throughout the production of a stronger exopolysaccharide matrix, which, in its turn, was corroborated by changes in cell surface electric charge.

The CLSM studies were performed at the Technical University of Munich, Germany. A.C.R. thanks L. Hendrickx for assistance in the labeling of *P. putida* and A. Schnell for help in flow-cell experiments.

References

APHA, WPCF. 1998. Standard methods for the examination of water and wastewater. Washington, DC: American Public Health Association.

Barkay T, Navon-Venezia S, Ron EZ, Rosenberg E. 1999. Enhancement of solubilization and biodegradation of polyaromatic hydrocarbons by the bioemulsifier alasan. Appl Environ Microbiol 65: 2697–2702.

Bastiaens L, Springael D, Wattiau P, Harms H, Wachter R, Verachtert H, Diels L. 2000. Isolation of adherent polycyclic aromatic hydrocarbon (PAH)-degrading bacteria using PAH-sorbing carriers. Appl Environ Microbiol 66:1834–1843.

Bezalel L, Hadar Y, Fu PP, Freeman JP, Cerniglia CE. 1996. Metabolism of phenanthrene by the white rotus fungus Pleurotus ostreatus. Appl Environ Microbiol 62:2547–2553.

Boldrin B, Tiehm A, Fritzsche C. 1993. Degradation of phenanthrene, fluorene, fluoranthene, and pyrene by a Mycobacterium sp. Appl Environ Microbiol 59:1927–1930.

Burd G, Ward OP. 1996. Involvement of a surface-active high-molecular-weight factor in degradation of polycyclic aromatic hydrocarbons by *Pseudomonas marginalis*. Can J Microbiol 42:791–797.

Cerniglia CE. 1992. Biodegradation of polycyclic aromatic hydrocarbons. Biodegradation 3:351–368.

Dubois M, Gilles KA, Hamilton JK, Rebers PA, Smith F. 1956. Colorimetric method for determining sugars and related substances. Anal Chem 28:350–356.

Dunn NW, Gunsalus IC. 1973. Transmissible plasmid coding early enzymes of naphthalene oxidation in *Pseudomonas putida*. J Bacteriol 114:974–979.

Figurski DH, Helinski ER. 1979. Replication of an origin-containing derivative of plasmid RK2 dependent on a plasmid function provided in trans. Proc Natl Acad Sci U S A 76:1648–1652.

George EJ, Neufeld RD. 1989. Degradation of fluorene in soil by fungus Phanerochaete chrysosporium. Biotechnol Bioeng 33:1306–1310.

Guerin WF, Boyd SA. 1992. Differential bioavailability of soil-sorbed naphthalene to two bacterial species. Appl Environ Microbiol 58: 1142–1152.

Hwu CS, Tseng SK, Yuan CY, Kulik Z, Lettinga G. 1996. Adsorption of long-chain fatty acids onto granular sludge and its effect on up-flow anaerobic sludge bed reactor operation. In: Proceedings of the 1st IAWQ Specialized Conference on Adsorption in Water Environment and Treatment Processes, 5–9 November, 1996, Shirahama, Wakayama, Japan. p 91–98.

Kuehn M, Hausner M, Bungartz HJ, Wagner M, Wilderer P, Wuertz S. 1998. Automated confocal laser scanning microscopy and semi-automated image processing for analysis of biofilms. Appl Environ Microbiol 64:4115–4127.

Lazarova V, Pierzo V, Fontvielle D, Manem J. 1994. Integrated approach for biofilm characterisation and biomass activity control. Water Sci Tech 29:345–354.

Lopes FA, Vieira MJ, Melo LF. 2000. Chemical composition and activity of a biofilm during the start-up of an airlift reactor. Water Sci Tech 41:105–111.

Lowry OH, Rosebrough NJ, Farr AL, Randall RJ. 1951. Protein measurements with the folin phenol reagent. J Biol Chem 193: 265–275.

Neu TR. 1996. Significance of bacterial surface-active compounds in interaction of bacteria with interfaces. Microbiol Rev 60:151–166.

Oliveira DR. 1992. Physico-chemical aspects of adhesion. NATO ASI Ser E 223:45–58.

Rattee ID, Breuer MM. 1974. The physical chemistry of dye adsorption. New York: Academic Press.

Rosenberg M, Gutnic D, Rosenberg E. 1980. Adherence of bacteria to hydrocarbons: a simple method for measuring cell-surface hydrophobicity. FEMS Microbiol Lett 9:29–33.

Sutherland IW. 2001. Biofilm exopolysaccharides: a strong and sticky framework. Microbiology 147:3–9.

Unge A, Tombolini R, Moller A, Jansson JK. 1996. Optimization of GFP as a marker for detection of bacteria in environmental samples. In: Hastings et al., editors. Bioluminescence and chemiluminescence: molecular reporting with photons. Woods Hole, MA: John Wiley & Sons.

van Loosdrecht MCM, Lyklema J, Norde W, Scraa G, Zehnder AJB. 1987. Electrophoretic mobility and hydrophobicity as a measure to predict the initial steps of bacterial adhesion. Appl Environ Microbiol 53: 1898–1901.

Wick LY, Munain AR, Springael D, Harms H. 2002. Responses of Mycobacterium sp. LB501T to the low bioavailability of solid anthracene. Appl Microbiol Biotechnol 58:378–385.

Wodzinski RS, Coyle JE. 1974. Physicalstate of phenanthrene for utilization by bacteria. Appl Microbiol 27:1081–1084.